

Aging and the time and frequency structure of force output variability

DAVID E. VAILLANCOURT¹ AND KARL M. NEWELL²

¹School of Kinesiology, University of Illinois at Chicago, Chicago, Illinois 60608; and ²Department of Kinesiology, The Pennsylvania State University, University Park, Pennsylvania 16802

Submitted 1 March 2002; accepted in final form 1 November 2002

Vaillancourt, David E., and Karl M. Newell. Aging and the time and frequency structure of force output variability. *J Appl Physiol* 94: 903–912, 2003; 10.1152/jappphysiol.00166.2002.—The present study examined the time and frequency structure of force output in adult humans to determine whether the changes in complexity with age are dependent on external task demands. Healthy young (20–24 yr), old (60–69 yr), and older-old (75–90 yr) humans produced isometric force contractions to constant and sine wave targets that also varied in force level. First, force variability on each force task increased with advancing age. Second, both time and frequency analysis showed that the structure of the force output in the old and older-old adults was less complex in the constant-force level task and more complex in the sine wave force task. Third, the alterations in force output with aging were primarily due to low-frequency bands <4 Hz. These results support the postulation that the observed increase or decrease in physiological complexity with aging is influenced by the relatively fast time scale of external task demands (Vaillancourt DE and Newell KM. *Neurobiol Aging* 23: 1–11, 2002).

spectral analysis; fractal analysis; motor control; nonlinear dynamics

AGING TENDS TO INDUCE A RANGE of performance decrements in the human motor system. A common finding is that the amount of motor variability increases in the healthy aging adult over a broad set of tasks (7, 22, 35, 36). Although consideration of the amount of variability is an important indicator of the aging neuromuscular system, the structure of motor variability also provides significant insight into system organization and motor control (11, 13, 20, 26). The purpose of this article was to examine the effects of aging and task demands on the structure of force output variability. Whereas there has been considerable work on the structure of cardiac and respiratory rhythms with aging and disease (17, 18, 20, 21, 23), less emphasis has been given to the organizational properties of physiological output from the motor system.

A central theory regarding the age-related structure of behavioral and physiological variability is the loss of “complexity” construct due to aging and disease (24).

The term complexity is related to the broader concepts of fractals and dynamics in disease (9) and aging (41, 42), in which behavioral and physiological systems change due to aberrations in their time and frequency structure. The time and frequency structure of physiological output has been operationally measured by applying multiple dependent variables from both fractal and nonlinear dynamic time series methodology (1, 14, 17, 18, 21, 27, 30). One application from this time series methodology for biology and medicine has been in discovering new clinical diagnostic and prognostic biomarkers for health, aging, and disease (for review see Refs. 24, 37). Indeed, previous work on patients with Parkinson’s disease has shown an alteration in the time and frequency structure of force tremor with increases in the severity of Parkinson’s disease (39); however, to date, there has been no systematic investigation of the time and frequency structure of force output with human aging.

In this paper, we test the loss of complexity hypothesis, which projects that there will be reduced time and frequency complexity of force output with aging (24). A contrasting view, however, is that tasks with different external demands would differentially influence the time and frequency complexity of force output as a function of human aging (37, 38). In particular, we test the hypothesis that, when the aging neuromuscular system adapts to perform a task of a continuous and constant-force output, there will be a decrease in the time and frequency complexity with aging. However, when the neuromuscular system is required to produce a repetitive sinusoidal force output, there will be an increase in the time and frequency complexity of force output. In this view, the physiological complexity of the force output as a function of age can be driven to either increase or decrease, according to the external task demands.

Previous studies on isometric force output have shown that specific processes related to physiological tremor and sensorimotor feedback oscillations occur in different frequency bands of force output (4–6, 33, 40). As a consequence, the time and frequency structure of force output was examined in different frequency

Address for reprint requests and other correspondence: D. E. Vaillancourt, School of Kinesiology (M/C 194), The Univ. of Illinois at Chicago, 901 West Roosevelt Rd., Chicago, IL 60608 (E-mail: court1@uic.edu).

The costs of publication of this article were defrayed in part by the payment of page charges. The article must therefore be hereby marked “advertisement” in accordance with 18 U.S.C. Section 1734 solely to indicate this fact.

bands to determine the neural processes most affected by human aging. In summary, it was of interest to understand the frequency structure of the force output that was influenced by aging, external task demands, and their interaction. It was anticipated that the findings would have direct implications for theory about the nature of change in physiological complexity with human aging.

METHODS

Participants

A total of 30 participants were assigned to three different age groups: young group ($n = 10$; range: 20–24 yr of age; mean: 22 ± 1 yr; 5 women and 5 men), old group ($n = 10$; range: 64–69 yr of age; mean: 67 ± 2 yr; 5 women and 5 men), and older-old group ($n = 10$; range: 75–90 yr of age; mean: 82 ± 5 yr; 5 women and 5 men). Twenty-nine of the thirty participants were right-hand dominant. The participants were naive to the purpose of the experiment, and all participants gave informed consent to all experimental procedures, which were approved by the local Institutional Review Board.

The three age groups consisted of moderately active individuals. Persons who were highly active were excluded from the study. Also, elderly persons who were considered frail were excluded from the study. Twelve of twenty participants in the two elderly groups were taking medication for the treatment of high blood pressure. The distribution of persons taking medication for high blood pressure was eight in the older-old group and four in the old group. None of the elderly participants reported having a neuromuscular or neuropsychiatric disease, nor did any of the participants have diabetes. Also, 12 of 20 elderly participants reported having arthritis, and each was taking medication for the condition. The distribution of persons reporting arthritis of the hand was seven in the older-old group and five in the old group. All participants remained on their normal medications during testing.

Apparatus

Participants were seated in a chair with their dominant forearm resting on a table (75 cm in height). The participant's dominant hand was pronated and lay flat on the table with the digits of the hand comfortably extended. Figure 1 depicts the setup, in which, along with the wrist, the third, fourth, and fifth phalanges were constrained from moving. The elbow position remained constant throughout the experimental session. Through abduction, the participant's lateral side of the index finger contacted the load cell (Entran ELFS-B3), 1.27 cm in diameter, which was fixated to the table. The load cell was located 36 cm from the participant's body midline. Analog output from the load cell was amplified through a Coulbourn type A (strain-gauge bridge) S72-25 amplifier at an excitation voltage of 10 V and a gain of 100. A computer-controlled 16-bit analog-to-digital (A/D) converter sampled the force output at 100 Hz. The smallest increment of change in force that the A/D board could detect was 0.0016 N. The force output was displayed on a video monitor located 48.6 cm from the participants' eyes and 100 cm from the floor. According to previous work from our laboratory, the display-to-control gain was set at 20 pixels per 1-N change in force for each participant.

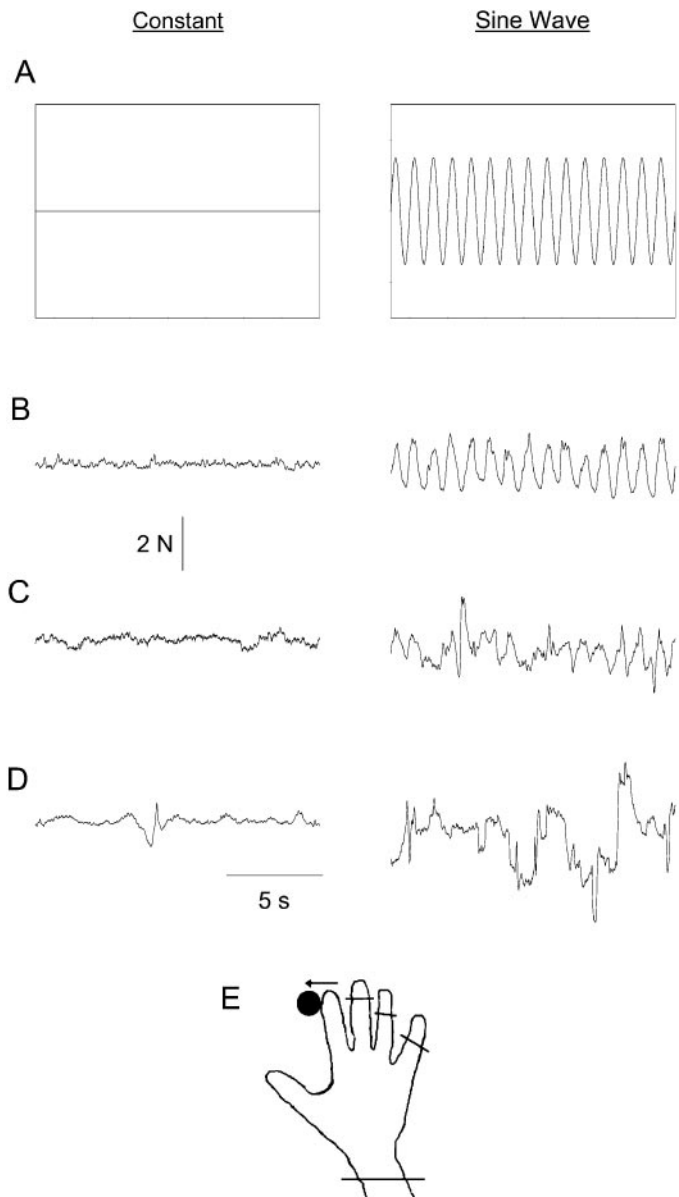


Fig. 1. Constant (left) and sine wave (right) force output task. A: the force target viewed by the participant. Force output is shown for a young (B), old (C), and older-old subject (D), respectively, at 10% maximum voluntary contraction (MVC). Subjects were instructed to match their force to the target line. E: hand setup during force production. The 3rd, 4th, and 5th phalanges were constrained from moving. Also, the wrist position was fixed throughout the session.

Procedures

During the initial portion of the experiment, the participant's maximum voluntary contraction (MVC) was estimated (40). Participants abducted their index finger against the load cell with maximal force for three consecutive 6-s trials. A 60-s rest period was provided for each participant between each MVC trial. In each MVC trial, the mean of the greatest 10 force samples was calculated. The means obtained from three trials were averaged to provide an estimate of each participant's MVC.

Participants adjusted their level of force output to match a red target line (1 pixel thick) on the video monitor. Participants viewed on-line feedback of their performance in the

form of a yellow force-time trajectory that moved from left to right in time across the video monitor (see Fig. 1). They were instructed to match the yellow trajectory line to the red horizontal target line throughout each trial and to minimize all deviations of the yellow line from the red line.

To examine task effects on the structure of force variability, participants produced force at a constant and sinusoidal target. The constant target was a horizontal line displayed across the center of the video monitor. The sinusoidal target consisted of a 1-Hz sine wave that spanned the width of the monitor. The amplitude of the target sine wave was 10% of the individual participant's MVC. Participants produced force at 5, 10, 20, and 40% of their MVC under both the constant and sine wave force conditions. They produced force for two consecutive 25-s trials at each unique condition. A rest period of 100 s was provided between each force trial. The order of the force and target conditions was randomized across all participants.

Data Analysis

The force-time series data were conditioned by the following methods. First, the initial 5 s of each force-time series were removed to allow participants time to achieve the force target. Second, force data were digitally filtered by using a fourth-order Butterworth filter with a low-pass cutoff frequency of 20 Hz. All data processing and subsequent time and frequency analyses were performed by using software written in Matlab (The MathWorks, Natick, MA). The analysis of force output focused on two primary issues: 1) the amount of force variability and 2) the structure of force variability.

Amount of force variability. The amount of force variability was assessed by calculating the root mean square (RMS) error. The equation

$$\text{RMSE} = \left[\frac{1}{N-1} \sum_{i=1}^N (x_i - t)^2 \right]^{1/2} \quad (1)$$

where N is the number of data points in the time series, t is the force target, and x_i is the force sample, calculates the average sum of squared deviations of the participant's force output from the target force line.

Structure of force variability. The structure of force variability was examined by using multiple time and frequency analyses. Approximate entropy (ApEn), spectral slope analysis, spectral degrees of freedom (DOF), and power spectral analysis methods were used to examine the force signal.

ApEn. To examine the time-dependent structure, the ApEn of the force output was calculated (27, 28, 29). ApEn returns a value between 0 and 2, and it reflects the predictability of future values in a time series based on previous values. For example, a sine wave has accurate short- and long-term predictability, and this corresponds to an ApEn value near 0. If varying amplitudes of white Gaussian noise are added to a sine wave, then ApEn would increase. This increases the uncertainty of making future time series predictions when random elements are added. For a completely random signal (namely, white Gaussian noise), each future value in the time series is independent and unpredictable from previous values, and the ApEn value tends toward 2. The same algorithm and parameter settings ($m = 2$; $r = 0.2 \times \text{standard deviation of the signal}$) were used here and in previous work (33).

DETRENDED FLUCTUATION ANALYSIS. The second time domain analysis used to assess the structure of force variability was the detrended fluctuation analysis (DFA), and the full details of the DFA method have been described elsewhere (12, 13).

Briefly, the force signal is first integrated and detrended. Next, the RMS is calculated at different time scales, and the slope of the relationship between the fluctuation magnitude and the time scale determines the fractal scaling index (α). We calculated DFA over the region $10 \leq n \leq 122$ (because each time step was 10 ms, this translates into 100 and 1,220 ms, respectively), where n is the length of each box (i.e., number of time bins in each box) designating where the linear regression fits were performed. The x -axis of Fig. 2 shows the logarithmic scale of the DFA calculated region where the \log_{10} of 10 equals 1 and \log_{10} of 122 is 2.0864.

Figure 2 shows plots from the DFA in the constant (Fig. 2A) and sine wave (Fig. 2B) tasks. The area between the vertical dashed line indicates where the linear regression was calculated. The average r^2 value between the $\log n$ and $\log F(n)$ across all subjects and conditions was 0.96 with a standard deviation of 0.01. The slopes were always calculated in the same region across subjects and task conditions. In the sine wave task, there was a crossover, but this element of the

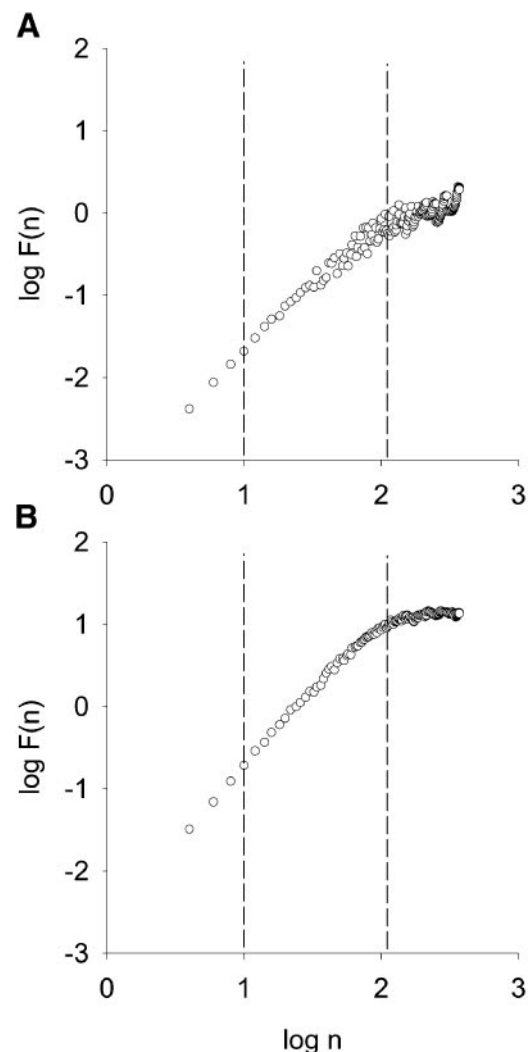


Fig. 2. Example plots from the detrended fluctuation analysis (DFA) method in the constant (A) and sine wave (B) tasks. The slope was calculated between the vertical dashed lines, and the average r^2 values between the $\log n$ and $\log F(n)$ across all subjects and conditions was 0.96 with a SD of 0.01. This scaling region was determined as the optimal scaling region based on previous work using the DFA method (12, 13, 16).

data was not included in the exponent estimate. Therefore, the slope estimates were taken over the optimal scaling region of the DFA plots (16).

If the force output fluctuations are random, then α would be closer to 0.5. In contrast, if the α value tends toward 1.5, this indicates that the data are consistent with brown noise. If the α value is closer to 1.0, this suggests that long-term correlations are present in the force data. It has previously been suggested that aging and disease are associated with either random noise or brown noise and that physiological variability from a healthy person is consistent with the presence of long-term correlations (10, 18).

FREQUENCY ANALYSIS. Several frequency analysis methods were used to quantify the frequency structure of the force signal. Before the frequency structure was quantified, the Fourier analysis method was applied to the force data (19). Autospectral analysis of the force signal was performed by using Welch's averaged periodogram method, with a window size of 256. Because the force signal was sampled at 100 Hz, this approximated a 0.3906-Hz frequency bin for each power spectral estimate.

The first frequency analysis statistic calculated was spectral DOF. Spectral DOF is a statistic that was initially introduced by Blackman and Tukey (2). Spectral DOF is calculated from

$$\text{DOF} = \frac{\left(\sum_i^N S_i \right)^2}{\sum_i^N S_i^2} \quad (2)$$

where S_i are the power estimates at each frequency bin. Note that the quantity is unity for a perfectly sharp peak and equal to N for white noise.

The second frequency analysis, the spectral slope, was calculated by the following equation

$$S = af^b \quad (3)$$

In this equation, the power function exponent, b , is a parameter that scales changes in spectral frequency, f , to changes in spectral power, S . When changes in power as a function of frequency are viewed graphically, b identifies the slope and a represents the y -intercept of the equation (8, 23). For the purposes of the present study, only the value of b was of interest. As the power spectrum becomes more broadband, and therefore closer to white Gaussian noise, the value of the

power function exponent increases from negative values toward zero. Thus, like ApEn, DFA, and the spectral DOF, the exponent of the power spectrum provides another means of obtaining a global description of the structure of force variability.

Because specific neurophysiological processes are related to the frequency structure of force output, the third frequency analysis used in this study examined the sum of the S in the 0- to 4-, 4- to 8-, and 8- to 12-Hz bins. Physiological tremor is present at higher frequencies between 5 and 12 Hz in the force recording (4, 5), and essentially all of the power related to slow sensorimotor (e.g., visuomotor) processing is located in the 0- to 4-Hz band of the force spectrum (6, 33, 40).

SURROGATE ANALYSIS. When using measures of complexity, it is important to rule out the possibility that changes in the dependent variable are merely a reflection of random noise (31, 34). To ensure that our data did not reflect a purely stochastic process, the random time shuffle technique was used. Twenty surrogate time series were constructed for each unique force condition for each participant. After each surrogate time series was constructed, ApEn, spectral DOF, and the spectral slopes were calculated on the surrogate data and then compared with the ApEn, spectral DOF, and spectral slope values from the original data, respectively. These methods are described in more detail in the RESULTS section and in Schreiber and Schmitz (31).

Statistics. The dependent variables described in the preceding sections were placed in repeated-measures ANOVA with a between-participant factor for age group and repeated measures on the task and force output conditions. The ANOVA was evaluated as significant when there was a <5% chance of making a type I error ($P < 0.05$). All statistical analyses were completed by using the Statistica statistical package (StatSoft).

RESULTS

Amount of Force Variability

Figure 1 shows force output from a young (B), old (C), and older-old (D) participant at 10% MVC at the constant and sine wave targets. The amount of force variability was examined by calculating the RMS on each trial.

Figure 3 depicts the RMS scores from each group across each unique condition, and it is clear that the amount of force variability increased with increases in

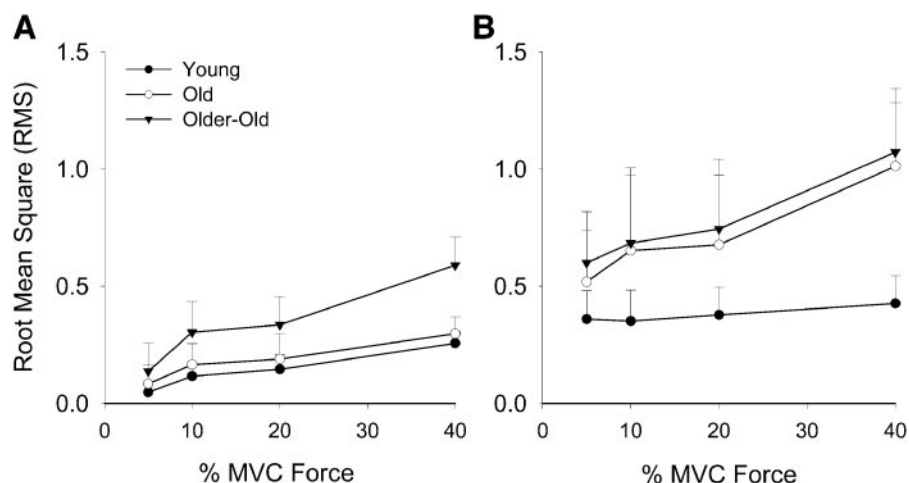


Fig. 3. Root-mean-square (RMS) values representing the amount of force variability in the constant and sine wave force task. ●, Young; ○, old; ▼, older-old group. Each symbol represents the average of all 10 subjects, and the error bars represent the between-subject SD.

the force target level. The ANOVA (aging \times task \times force) confirmed that the RMS increased with the force target level [$F(3,81) = 22.76, P < 0.01$] and increased from the constant to the sine wave target [$F(1,27) = 45.45, P < 0.01$]. As shown in Fig. 3, the old and older-old groups had greater RMS values at each force level compared with the younger participants, and this resulted in a significant main effect for age [$F(2,27) = 11.57, P < 0.01$]. In addition, there was a significant age-by-task interaction [$F(2,27) = 4.62, P < 0.01$], an age-by-force target interaction [$F(6,81) = 3.28, P < 0.01$], a task-by-force interaction [$F(3,81) = 4.36, P < 0.01$], and a three-way age-by-task-by-force interaction [$F(6,81) = 2.38, P < 0.05$].

Additional two-way (age \times task) ANOVA was performed at each of the four force levels to determine whether the effects of aging occurred at each force level. At 5% MVC, there were greater RMS values with aging, which resulted in a main effect for age, [$F(2,27) = 14.14; P < 0.0001$], and the effect for task was also significant [$F(1,27) = 109.42; P < 0.0000$]. None of the interactions reached significance. Tukey's honestly significant different (HSD) post hoc test revealed that the old and older-old groups had significantly greater RMS values compared with the young group, but there was no statistically significant difference between the two older age groups. At 10% MVC, the RMS values were greater in the old and older-old groups [$F(2,27) = 9.35; P < 0.0008$], and the sine wave task had greater RMS values than the constant task [$F(1,27) = 70.85; P < 0.0000$]. None of the interactions reached significance. Similar to the 5% force level, Tukey's HSD post hoc test revealed that the old and older-old groups were different from the young group but not different from each other. At 20% MVC, the main effect for aging was significant [$F(2,27) = 17.29; P < 0.0000$], and the task main effect was again highly significant [$F(1,27) = 27.00; P < 0.0000$]. None of the interactions reached significance. Tukey's HSD post hoc test again revealed that the old and older-old groups were different from the young group. In contrast to the 5 and 10% MVC conditions, in the 20% MVC condition the older-old group had greater RMS values than the old group. Finally, at 40% MVC, the RMS values were significant for age group [$F(2,27) = 5.17; P < 0.0126$] and for the sine wave having greater RMS values compared with the constant-force task [$F(1,27) = 17.42; P < 0.0003$]. The age-by-task interaction did approach significance [$F(2,27) = 3.28; P < 0.0529$], but none of the other interactions were significant. Tukey's HSD post hoc test revealed that the old and older-old groups were different from the young group, but there were no significant differences between the two old-age groups.

Taken together, these results indicate that force variability (RMS) was greater for the older individuals compared with the young individuals at each force level. At three of four force levels (5, 10, and 40%), there was no statistically significant difference between the two old-age groups, but Fig. 3 does suggest

small differences. There was also a consistently higher level of force variability in the sine wave task compared with the constant-force task. Finally, the three-way age-by-task-by-force interaction was shown to be the product of an age-by-task interaction at the 40% MVC force level, whereas there was no age-by-task interaction at the other force levels.

Structure of Force Variability

To determine whether the force data showed any nonstationarity during the trial, the mean and standard deviation of force output were calculated for the first and second half of each trial and compared in a three-way (age \times initial/last \times task) ANOVA for each force level. Neither the mean nor the standard deviation of force was different between the first and second half of the force time series. This result indicates that nonstationarity was not a limiting factor in the time series analyses that follow.

Figure 4 shows the force output in the sine wave and constant-force task along with the log-log plot from spectral analysis. The data reveal opposite trends for the spectral slope with aging in the constant compared with the sine wave task. This phenomenon was assessed in the time and frequency domains by using ApEn, DFA, spectral DOF, and spectral slope analyses. Figure 5A shows that, in the constant task, ApEn decreased across the young, old, and older-old groups but that it increased with aging in the sine wave task. These directionally opposite changes in ApEn across task and age group resulted in a nonsignificant main effect in the ANOVA for age [$F(2,27) = 0.77, P > 0.05$], but there was a significant decrease in ApEn from the constant task to the sine wave task [$F(1,27) = 99.96, P < 0.01$]. The observation of directionally opposite changes in ApEn with task and age was confirmed by a highly significant age-by-task interaction [$F(2,27) = 17.03, P < 0.01$]. Two separate ANOVAs (aging \times force) were calculated for the constant and sine wave force task, which revealed a significant decrease in ApEn across aging in the constant task [$F(2,27) = 4.81; P < 0.01$] and a significant increase in ApEn across aging in the sine wave task [$F(2,27) = 3.62, P < 0.05$]. The ApEn analysis revealed that the structure of force output was more regular in the sine wave task compared with the constant task and, most importantly, that there is more regular force contractions in the constant-force task and more irregular force contractions in the sine wave task with advancing age.

Figure 5B shows the scaling index α from the DFA method in the constant and sine wave tasks. The α value increases with aging in the constant-force task and decreases with aging in the sine wave force task. This finding resulted in a nonsignificant main effect for age [$F(2,27) = 0.38, P > 0.05$], but there was a significant increase in α from the constant to the sine wave task [$F(2,27) = 47.84, P < 0.01$]. The opposite changes in the scaling index α with age between the two tasks resulted in an age-by-task interaction [$F(2,27) = 21.69, P < 0.01$]. We calculated two separate ANOVAs (ag-

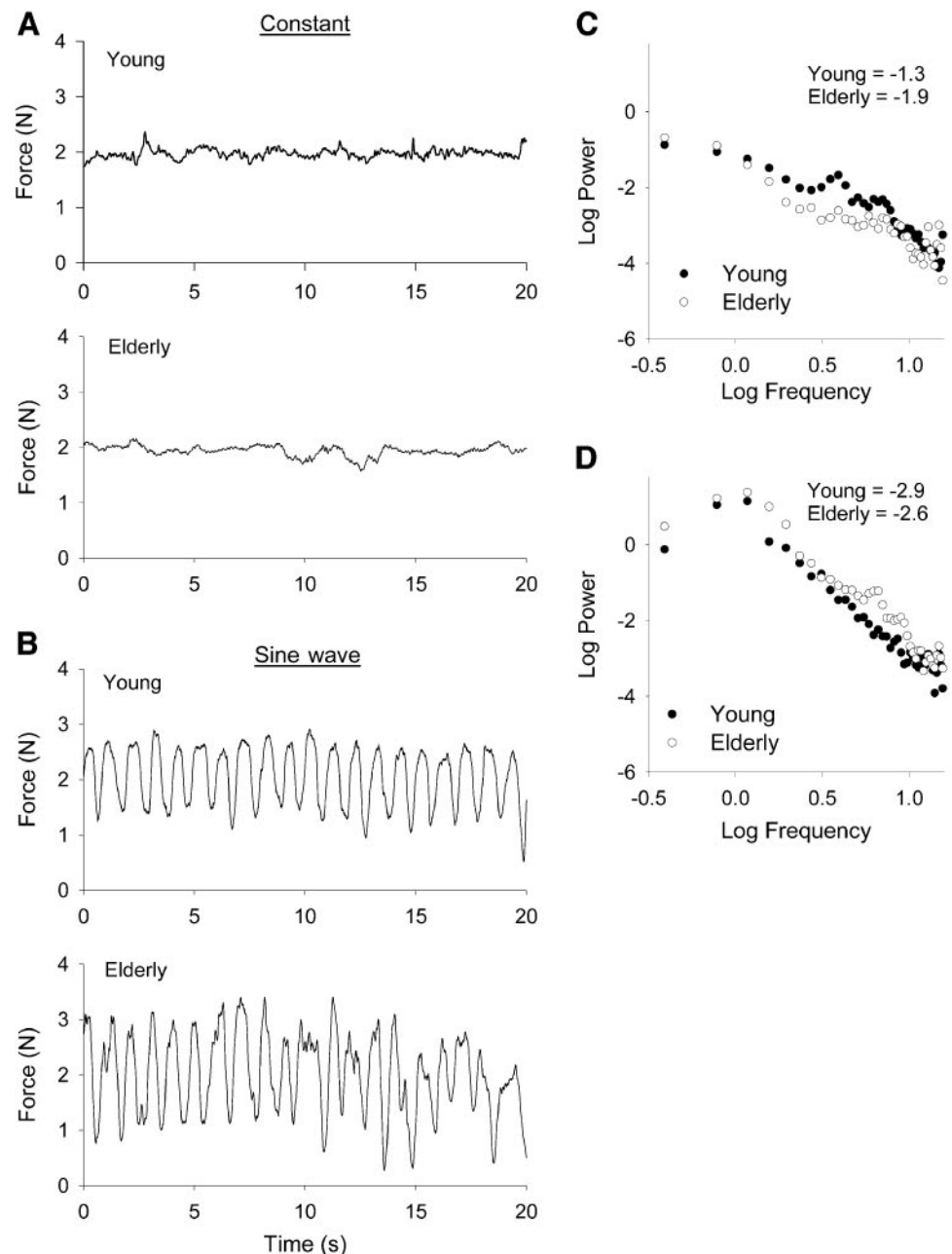


Fig. 4. Force output and the spectral slope analysis in the constant and sine wave tasks. **A:** force output from a male young subject (25 yr; *top*) and male older-old subject (78 yr; *bottom*) in the constant-force task. **C:** the corresponding log-log spectral analysis plot, where the slope for the young subject was -1.3 and that for the older-old subject was -1.9 . **B:** the force output from the same 2 subjects in the sine wave force task. **D:** the corresponding log-log spectral analysis plot. The opposite trend is observed with the younger subject having a more negative slope, -2.9 , compared with the older-old subject, -2.6 .

ing \times force) for the constant and sine wave force task, which revealed a significant increase in α across aging in the constant task [$F(2,27) = 3.6$, $P < 0.05$] and a significant decrease in α across aging in the sine wave task [$F(2,27) = 18.41$, $P < 0.01$]. The DFA analysis revealed that there was more Brownian noise with aging in the constant task but that the pattern reversed with more Brownian noise in the younger group in the sine wave task.

The spectral DOF analysis examines the structure of the force oscillations in the frequency domain where higher values correspond to more spectral DOF. Figure 5C shows that the spectral DOF values decreased with advancing age in the constant task and increased with advancing age in the sine wave task, and this resulted

in a nonsignificant main effect for age [$F(2,27) = 0.18$, $P > 0.05$]. There was, however, a significant decrease in spectral DOF from the constant task to the sine wave task [$F(1,27) = 87.28$, $P < 0.01$]. The important finding from the ANOVA was that there was a significant aging-by-task interaction [$F(2,27) = 18.05$, $P < 0.01$]. Two separate (aging \times force) ANOVAs were calculated for each task, and there was a significant decrease [$F(2,27) = 3.53$, $P < 0.05$] and increase [$F(2,27) = 20.53$, $P < 0.05$] in spectral DOF with aging in the constant and sine wave tasks, respectively. Thus the spectral DOF results revealed that the frequency structure of the force output had fewer spectral DOF with aging in the constant-force task and greater spectral DOF with aging in the sine wave task.

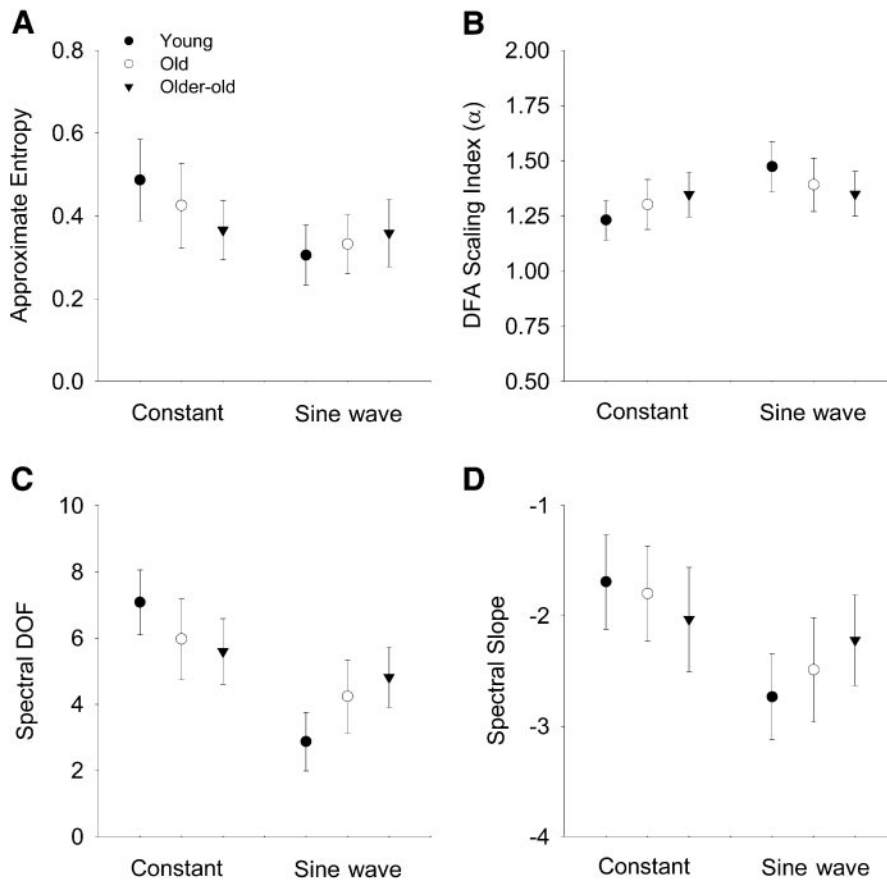


Fig. 5. Structure of force output variability. Time and frequency analyses are shown with the use of approximate entropy (A), DFA (B), spectral degrees of freedom (DOF; C), and the spectral slope analysis (D) (1, 2, 11, 13, 29). ●, Young; ○, old; ▼, older-old group. Each symbol represents the average of all 10 subjects collapsed across all 4 force levels, and the error bars represent the SD.

The spectral slope was calculated by estimating the slope from the best-fitted linear regression between the log-log relation of the frequency and power axes from Fourier analysis. Figure 5D shows that the spectral slope became more negative with aging in the constant task and more positive with aging in the sine wave task. The ANOVA also confirmed that there was a significant aging-by-task interaction [$F(2,27) = 7.33$, $P < 0.01$]. The ANOVA revealed that there were more negative spectral slopes for the sine wave task compared with the constant-force task [$F(1,27) = 222.11$, $P < 0.01$]. In summary, the ApEn, DFA, spectral DOF, and spectral slope analyses showed systematic task-dependent differences in the structure of force output complexity with aging.

An important concept when using measures of complexity is to rule out the possibility that changes in the dependent variable are merely a reflection of random noise (31, 34). To ensure that our data did not reflect a purely stochastic process, the random time shuffle technique was used. In performing the surrogate tests, 20 surrogate time series were constructed for each unique force condition for each participant. After each surrogate time series was constructed, ApEn, DFA, spectral DOF, and the spectral slopes were calculated on the surrogate data and then compared with the ApEn, DFA, spectral DOF, and spectral slope values from the original data. The null hypothesis tested in this analysis is that the original data are consistent

with a purely stochastic process. If the original data were consistent with a purely stochastic model, then we would expect similar statistical values in the surrogate data compared with the original time series.

We calculated the statistic S

$$S = |M_{\text{orig}} - M_{\text{surr}}| / \text{SD}_{\text{surr}} \quad (4)$$

where M_{orig} is the original ApEn, DFA, spectral DOF, or spectral slope value; M_{surr} is the surrogate ApEn, DFA, spectral DOF, or spectral slope value; and SD_{surr} is the standard deviation of the ApEn, DFA, spectral DOF, or spectral slope values from the 20 surrogate time series. The value S from Eq. 4 represents the number of standard deviations separating the original from the surrogate statistic. Thus the higher the S value, the more robust the difference between the original data and its surrogates. If the null hypothesis were true, then we would expect very low S values near zero. Table 1 shows the mean and standard deviation of the S values for each group for ApEn, DFA, spectral DOF, and the spectral slope. The S values were clearly greater than zero for each participant, and the standard deviation values did not approach zero. Thus the null hypothesis that the original data are consistent with a purely stochastic process can be rejected.

Frequency Structure of Force Output

Specific neurophysiological processes are related to the frequency structure of force output. We examined

Table 1. Mean spectral power values from surrogate analysis

	ApEn	DFA Scaling Index α	Spectral DOF	Spectral Slope
Young	82.8 \pm 20.9	17.7 \pm 4.0	16.8 \pm 3.6	13.1 \pm 4.4
Old	85.5 \pm 17.9	17.5 \pm 4.1	15.9 \pm 2.9	12.9 \pm 4.1
Older-old	86.7 \pm 12.3	16.8 \pm 3.7	16.4 \pm 3.1	12.7 \pm 3.6

Values are means \pm SD. ApEn, approximate entropy; DFA, detrended fluctuation analysis; DOF, degrees of freedom.

the sum of power in the 0- to 4-, 4- to 8-, and 8- to 12-Hz frequency bands of force output to determine whether the differences found in the variability analyses with aging are related to visuomotor control or to changes in physiological tremor.

Figure 6A shows the spectral analysis of force output from a young, old, and older-old participant in the constant-force task at 20% MVC. Essentially all of the power for each participant is located in the 0- to 4-Hz band, and there were systematic differences among the participants in this frequency band. The older-old participants had the greatest power compared with the old and young participants, with the peak power \sim 1 Hz. The old participants had a higher amount of power in the 0- to 2-Hz band compared with the young participants, and the peak power for each participant was also \sim 1 Hz. Two separate three-way [aging \times force \times frequency bin (0–4, 4–8, 8–12 Hz)] ANOVAs for the constant and sine wave task were used to examine the significant changes in power in the different frequency bins.

Figure 6B shows the results from the constant-force task that is consistent with Fig. 6A, showing that most of the differences between the aging groups were located in the 0- to 4-Hz band of force output. In the constant-force task, the ANOVA revealed a significant

increase in the sum of power with aging [$F(2,27) = 7.26$, $P < 0.01$]; there was an increase in the sum of power with increased force output level [$F(3,81) = 29.35$, $P < 0.01$] and a significant decrease in power from the 0- to 4- to the 4- to 8- and 8- to 12-Hz bands [$F(2,54) = 59.51$, $P < 0.01$]. The sine wave force task revealed similar main effects for aging, force, and frequency bins [$F(2,27) = 4.79$, $P < 0.05$; $F(3,81) = 5.53$, $P < 0.01$; $F(2,54) = 33.26$, $P < 0.01$]. The important observation from the ANOVA was a significant aging-by-frequency bin interaction in both the constant [$F(4,54) = 7.53$, $P < 0.01$] and sine wave tasks [$F(4,54) = 2.83$, $P < 0.05$], and planned contrast analysis directly showed that the interactions were due to aging differences in the 0- to 4-Hz bandwidth (also see Fig. 6B).

DISCUSSION

The purpose of this study was to examine the structure (in the time and frequency domains) of force output variability as a function of human aging. However, it is important to note that the findings from both force output tasks were clear in showing the traditional effect of the amount of force variability being higher in the old and older-old groups compared with the young participants. Although previous reports on continuous isometric force production at the knee extensors have not found differences in force variability with age (3, 15), the age-related variability differences found in this study are consistent with previous reports examining the effects of aging on the amount of isometric force variability at the first dorsal interosseus during second-finger abduction (7, 22, 36). This difference in force variability with aging found at different muscle groups could be related to use and disuse or to the natural changes in the neuromuscular system at different joints with aging. Another difference found in this

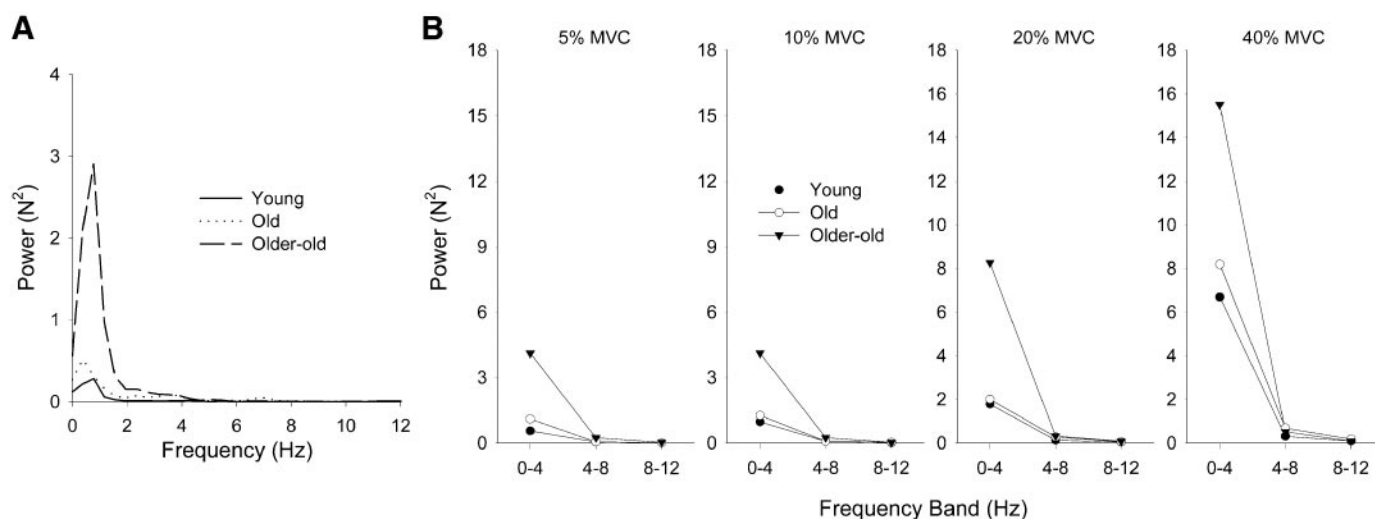


Fig. 6. Sum of power (N^2) for the young, old, and older-old subjects in the constant-force task. A: individual subject power spectrum for a young (solid line), old (dotted line), and older-old (dashed line) subject at 20% MVC. B: sum of power across force levels and the 0- to 4-, 4- to 8-, and 8- to 12-Hz frequency bins. The sum of power was calculated by summing the total power at each 0.3906-Hz bin for each unique condition. ●, Young; ○, old; ▲, older-old group. Each symbol is the average across 10 subjects in the constant-force task at each unique condition.

study compared with previous work was that we found greater differences with age at the highest force levels compared with the lower force levels. Whereas this finding may seem counter to previous studies (7, 22), this is likely due to the previous work normalizing the force variability to the mean force produced (i.e., coefficient of variation). For example, in a separate study with the same participants, we showed that, in the coefficient of variation, the largest differences between age groups is observed at the lowest force levels (36), and a similar observation for the standard deviation and the coefficient of variation can be seen in the data from other laboratories in the literature (Fig. 3 in Ref. 22).

The findings from the amount of force variability also showed an age-by-task interaction, with greater differences found between the age groups in the sine wave task compared with the constant-force task. This finding is consistent with previous data that showed that, during knee extension, older persons produce greater force output variability in discrete force contractions, but there are no differences with aging for continuous force contractions (3). In our task, sine wave force control is similar to the discrete force contractions, and these two studies provide converging evidence that older persons are more variable during ballistic or discrete force contractions than during continuous force control.

The time and frequency complexity of force output was assessed through analyses using ApEn, DFA, spectral DOF, and spectral slope analysis to examine the structure of force output (1, 2, 11, 13, 27). The analyses showed that all of these indexes of force output changed in parallel, showing less complex force contractions with aging in the constant-force task and more complex force contractions with aging in the sine wave force task. The finding of an interaction between the constant or sine wave task and aging is counter to the hypothesis that would project that the complexity of force output always decreases with aging (24). The surrogate data analysis showed that the increase and decrease in the time and frequency complexity were not due to alterations in stochastic, uncorrelated noise (10, 34, 38), and this provides confidence in the robustness of the challenge that these data provide to the loss of complexity hypothesis.

The findings from these experiments are much more consistent with the hypothesis that the directional change in behavioral and physiological complexity with aging is not a universal relation but rather is, to some degree, dependent on external demands (37). In particular, in physiological and behavioral systems in which the task dynamic is a dimension of zero (fixed-point attractor), there will be a decrease in complexity with aging and disease. This is because, to realize the task goal of no motion, additional DOF are introduced by the neuromuscular system, but older adults are poorer at this (hence lower complexity) than their younger counterparts. In contrast, there is an increase in complexity with aging and disease in systems in which the task dynamic is oscillatory, and older adults

have more difficulty reducing the dimension of their output to a lower dimension than the intrinsic dynamics of the resting state of the system (37, 41, 42). The present findings provide support for this hypothesis by showing less complex force output with aging in the constant (fixed-point) task and more complex force output in the sine wave (oscillatory) task.

Physiological output is due to the interaction of the confluence of constraints from the organism, environment, and task (25). Clearly, the processes of aging induce a variety of changes to the system (organism), but they are typically always assessed in the context of a particular environment and task demands. Thus it is very difficult to derive an isolated test of the aging system from the perspective of the organism alone. The different sources of constraint to human aging also tend to have different time scales or rates of change in their influence on the neuromuscular system. The processes that are typically associated with aging tend to have slower rates of change than those that can be induced by external task demands that require a rapid change from the resting stable state of the system. Thus the aging system itself may be on a slow decline to reduced complexity (24), but this assessment is typically mediated and sometimes masked by the demands of the task (37).

Another important finding from this paper was that the alterations in the time and frequency structure were due to changes in the low-frequency, rather than high-frequency, portion of force output. Previous studies on isometric force output have shown that specific processes related to physiological tremor and sensorimotor feedback oscillations occur in different frequency bands (6). For instance, processes related to physiological tremor are present at higher frequencies between 5 and 12 Hz in the force recording (5), and essentially all of the power related to sensorimotor processing is located in the 0- to 4-Hz band of the force spectrum (33, 40). In this context, most of the changes in force output variability with human aging occur through slow sensorimotor processes. It is evident that several sensory and motor processes could potentially mediate the present findings (22, 32, 36).

In summary, this study showed three key findings. First, the amount of force variability was found to increase with aging at each force level examined. Also, the sine wave force contractions were more variable than the constant-force contractions, consistent with previously reported findings at the knee joint (3). Second, this paper provides the first direct empirical evidence that the force output signal from the second-finger abduction can increase or decrease in complexity with aging, depending on the constant or sine wave task. These findings support the theoretical position advanced regarding increases and decreases in biological signal complexity with human aging and disease (37). Third, the spectral analysis directly showed that changes in force output observed with human aging were primarily due to alterations in the low 0- to 4-Hz band of the force output signal.

This research was supported in part by National Institute on Aging Grant T32-AG00048, the Gerontology Center at The Pennsylvania State University Grant GERO 423-141001, and Grants-in-Aid Research from the National Academy of Sciences through Sigma Xi. We also thank the nursing care staff of The Pennsylvania State General Clinical Research Center at the Noll Physiological Research Laboratory (Division of Research Resources Grant M01-RR-10732).

REFERENCES

1. **Bassingthwaighte JB, Liebovitch LS, and West BJ.** *Fractal Physiology*. New York: Oxford Univ. Press, 1994.
2. **Blackman RB and Tukey JW.** *The Measurement of Power Spectra: From the Point of View of Communications Engineering*. New York: Dover, 1958.
3. **Christou EA and Carlton LG.** Old adults exhibit greater motor output variability than young adults only during rapid discrete isometric contractions. *J Gerontol A Biol Sci Med Sci* 56: B524–B532, 2001.
4. **Elble RJ and Koller WC.** *Tremor*. Baltimore, MD: Johns Hopkins University Press, 1990.
5. **Elble RJ and Randall JE.** Motor unit activity responsible for 8–12 Hz component of human physiological finger tremor. *J Neurophysiol* 39: 370–383, 1976.
6. **Freund HJ and Hefter H.** The role of the basal ganglia in rhythmic movement. In: *Advances in Neurology*, edited by Narabayashi H, Nagatsu T, Yanagisawa Y, and Mizuno Y. New York: Raven, 1993, vol. 60, p. 88–92.
7. **Galganski ME, Fuglevand AJ, and Enoka RM.** Reduced control of motor output in a human hand muscle of elderly participants during submaximal contractions. *J Neurophysiol* 69: 2108–2115, 1993.
8. **Gilden DL, Thornton T, and Mallon MW.** 1/f Noise in human cognition. *Science* 267: 1837–1839, 1995.
9. **Glass L.** Synchronization and rhythmic processes in physiology. *Nature* 410: 277–284, 2001.
10. **Goldberger AL, Peng CK, and Lipsitz LA.** What is physiological complexity and how does it change with aging and disease? *Neurobiol Aging* 23: 23–26, 2002.
11. **Goldberger AL and West BJ.** Fractals in physiology and medicine. *Yale J Biol Med* 60: 421–435, 1987.
12. **Hausdorff JM, Mitchell SL, Firtion R, Peng CK, Cudkowicz ME, Wei JY, and Goldberger AL.** Altered fractal dynamics of gait: reduced stride interval correlations with aging and Huntington's disease. *J Appl Physiol* 82: 262–269, 1997.
13. **Hausdorff JM, Peng CK, Ladin Z, Wei JY, and Goldberger AL.** Is walking a random walk? Evidence for long-range correlations in stride interval of human gait. *J Appl Physiol* 78: 349–358, 1994.
14. **Heath RA.** *Nonlinear Dynamics: Techniques and Applications to Psychology*. Mahwah, NJ: Erlbaum, 2000.
15. **Hortobagyi T, Tunnel D, Moody Beam S, and DeVita P.** Low- or high-intensity strength training partially restores impaired quadriceps force accuracy and steadiness in aged adults. *J Gerontol A Biol Sci Med Sci* 56: B38–B47, 2001.
16. **Hu K, Ivanov PC, Chen Z, Carpena P, and Eugene SH.** Effect of trends on detrended fluctuation analysis (Abstract). *Phys Rev E Stat Phys Plasmas Fluids Relat Interdiscip Topics* 64: 011114, 2001.
17. **Ivanov PC, Amaral LAN, Goldberger AL, Havlin AL, Havlin S, Rosenblum MG, Struzik Z, and Stanley HE.** Multifractality in human heartbeat dynamics. *Nature* 399: 461–465, 1999.
18. **Iyengar N, Peng CK, Raymond M, Goldberger AL, and Lipsitz LA.** Age-related alterations in the fractal scaling of cardiac interbeat interval dynamics. *Am J Physiol Regul Integr Comp Physiol* 271: R1078–R1084, 1996.
19. **Jenkins GM and Watts DG.** *Spectral Analysis and Its Applications*. London: Holden-Day, 1968.
20. **Kaplan DT, Furman MI, Pincus SM, Ryan SM, Lipsitz LA, and Goldberger AL.** Aging and the complexity of cardiovascular dynamics. *Biophys J* 59: 945–949, 1991.
21. **Kresh JY and Izrailtayan I.** Evolution in functional complexity of heart rate dynamics: a measure of cardiac allograft adaptability. *Am J Physiol Regul Integr Comp Physiol* 275: R720–R727, 1998.
22. **Laidlaw DH, Bilodeau M, and Enoka RM.** Steadiness is reduced and motor unit discharge is more variable in old adults. *Muscle Nerve* 23: 600–612, 2000.
23. **Lipsitz LA.** Age-related changes in the “complexity” of cardiovascular dynamics: a potential marker of vulnerability to disease. *Chaos* 5: 102–109, 1995.
24. **Lipsitz LA and Goldberger AL.** Loss of “complexity” and aging: potential applications of fractals and chaos theory to senescence. *JAMA* 267: 1806–1809, 1992.
25. **Newell KM.** Constraints on the development of coordination. In: *Motor Skill Acquisition in Children: Aspects of Coordination and Control*, edited by Wade MG and Whiting HTA. Amsterdam: Martinus Nijhoff, 1986.
26. **Newell KM and Corcos DM (Editors).** *Variability and Motor Control*. Champaign, IL: Human Kinetics, 1993.
27. **Pincus SM.** Approximate entropy as a measure of system complexity. *Proc Natl Acad Sci USA* 88: 2297–2301, 1991.
28. **Pincus SM and Goldberger AL.** Physiological time-series analysis: what does regularity quantify? *Am J Physiol Heart Circ Physiol* 266: H1643–H1656, 1994.
29. **Pincus SM and Singer BH.** Randomness and degrees of irregularity. *Proc Natl Acad Sci USA* 93: 2083–2088, 1996.
30. **Richman JS and Moorman JR.** Physiological time-series analysis using approximate entropy and sample entropy. *Am J Physiol Heart Circ Physiol* 278: H2039–H2049, 2000.
31. **Schreiber T and Schmitz A.** Surrogate time series. *Phys Rev Lett* 142: 346–382, 2000.
32. **Seidler-Dobrin RD and Stelmach GE.** Persistence in visual feedback control by the elderly. *Exp Brain Res* 119: 467–474, 1998.
33. **Slifkin AB, Vaillancourt DE, and Newell KM.** Intermittency in the control of continuous force production. *J Neurophysiol* 84: 1708–1718, 2000.
34. **Theiler J, Eubank S, Longtin A, Galdrikian B, and Farmer JD.** Testing for nonlinearity in time series: the method of surrogate data. *Physica D* 58: 77–94, 1992.
35. **Tracy BL and Enoka RM.** Older adults are less steady during submaximal isometric contractions with the knee extensor muscles. *J Appl Physiol* 92: 1004–1012, 2002.
36. **Vaillancourt DE, Larsson L, and Newell KM.** Effects of aging on force variability, motor unit discharge patterns, and the structure of 10, 20, and 40 Hz EMG activity. *Neurobiol Aging* 24: 25–35, 2003.
37. **Vaillancourt DE and Newell KM.** Changing complexity in human behavior and physiology through aging and disease. *Neurobiol Aging* 23: 1–11, 2002.
38. **Vaillancourt DE and Newell KM.** Response to reviewer commentaries. *Neurobiol Aging* 23: 27–29, 2002.
39. **Vaillancourt DE, Slifkin AB, and Newell KM.** Regularity of force tremor in Parkinson's disease. *Clin Neurophysiol* 112: 1594–1603, 2001.
40. **Vaillancourt DE, Slifkin AB, and Newell KM.** Intermittency in the visual control of force in Parkinson's disease. *Exp Brain Res* 138: 118–127, 2001.
41. **Yates FE.** The dynamics of adaptation in living systems. In: *Adaptive Control of Ill-defined Systems*, edited by Selfridge OG, Rissland EL, and Arbib MA. New York: Plenum, 1984.
42. **Yates FE.** The dynamics of aging and time: how physical action implies social action. In: *Emergent Theories of Aging*, edited by Birren JE and Bengtson VL. New York: Springer, 1988.